Human periosteal derived cell expansion in a perfusion bioreactor system: Proliferation, differentiation and extracellular matrix formation

Short title: human periosteal derived cell expansion in a perfusion bioreactor system

Sonnaert, M.[1,2], Papantoniou, I.[1,3], Bloemen, V.[1,4], Kerckhofs, G.[1, 2, 5], Luyten, F.P.[1, 3], Schrooten, J.[1, 2*]

[1]Prometheus, Division of Skeletal Tissue Engineering, KU Leuven, Onderwijs en Navorsing 1 (+8), Herestraat 49 - PB813, B-3000 Leuven, Belgium.

[2]Department of Materials Engineering, KU Leuven, Kasteelpark Arenberg 44 – PB 2450, B-3001 Heverlee, Belgium.

[3]Skeletal Biology and Engineering reseach center, KU Leuven, Onderwijs en Navorsing 1, Herestraat 49 - PB813, B-3000 Leuven, Belgium.

[4]Biomedical Engineering Research team, Groep T, Leuven Engineering College (Association KU Leuven), Andreas Vesaliusstraat 13, B-3000 Leuven, Belgium

[5]Biomechanics Research Unit, Université de Liege, Chemin des Chevreuils 1 - BAT 52/3, B-4000 Liège, Belgium.

* correspondance to J.Schrooten, Prometheus, Division of Skeletal Tissue Engineering, KU Leuven, Onderwijs en Navorsing 1 (+8), Herestraat 49 - PB813, B-3000 Leuven, Belgium. E-mail : jan.schrooten@mtm.kuleuven.be

Abstract

Perfusion bioreactor systems have shown to be a valuable tool for the *in vitro* development of 3D cell-carrier constructs. Their use for cell expansion is however much less explored. Since maintenance of the initial cell phenotype is essential in this process, it is imperative to get an insight in the bioreactor-related variables determining cell fate. Therefore, this study investigated the influence of fluid flow induced shear stress on the proliferation, differentiation and matrix deposition of human periosteal derived cells in the absence of additional differentiation inducing stimuli. 120 000 cells were seeded on additive manufactured 3D Ti6Al4V scaffolds and cultured up to 28 days at different flow rates ranging between 0.04 and 6 ml/min. DNA measurements showed on average a threefold increase in cell content for all perfused conditions in comparison to static controls whereas the magnitude of the flow rate did not have an influence. Contrast-enhanced nanofocus X-ray computed tomography showed substantial formation of an engineered neo-tissue in all perfused conditions, resulting in a filling up to 70% of the total internal void volume and no flow-rate dependent differences were observed. The expression of key osteogenic markers such as RunX2, OCN, OPN and Col1 did not show any significant changes in comparison to static controls after 28 days of culture, with the exception of Osx at high flow rates. We therefore concluded that, in the absence of additional osteogenic stimuli, the investigated perfusion conditions increased cell proliferation but did not significantly enhance osteogenic differentiation thus allowing for this process to be used for cell expansion.

Keywords: bioreactor, perfusion, human periosteal derived cells, tissue engineering, cell expansion, nano CT, 3D

1. Introduction

The development of cell-based regenerative therapies to treat defects in the body is rapidly evolving (Martin *et al.* 2011; Martin *et al.* 2012). However, the translation of these techniques to a clinical setting still remains a major challenge due to suboptimal cell culture strategies leading to low yields of progenitor cells (Rodrigues *et al.* 2011). To address this, the development of robust processes using three dimensional (3D) bioreactor culture systems is a promising prospective (Grayson *et al.* 2004; Martin *et al.* 2004; Haycock 2011; Rodrigues *et al.* 2011; Jakob *et al.* 2012; Salter *et al.* 2012). Bioreactors play a crucial role in establishing and maintaining 3D cell culture, controlling and monitoring physicochemical parameters in the system as well as automating manual procedures (Martin *et al.* 2010). Next to this, these systems allow to exert controlled mechanical stimuli such as hydrostatic pressure and shear stress (SS) on the developing construct (i.e. combination of a 3D carrier and cells/extracellular matrix (ECM)), which can be used to guide cell behaviour (McCoy and O'Brien 2010; Salter *et al.* 2012).

Bioreactor facilitated stem cell expansion has already been achieved using multiple systems ranging from multi-layered cell factories to micro-carriers in stirred tank bioreactors (Jung *et al.* 2012). Different groups have already shown that the stem cell phenotype can be maintained in these systems despite the external hydrodynamic stresses applied on the cells by fluid flow during culture (Hewitt *et al.* 2011; Chang *et al.* 2012; Jung *et al.* 2012). However, despite the 3D shape of the carriers used in these systems, cells predominantly grow in a monolayer which does not reproduce the native environment of the cells (Haycock 2011). Additionally, the use of these systems does not stimulate ECM formation although its presence in a 3D architecture has been shown

to restrain spontaneous differentiation and preserve differentiation potential (Chen *et al.* 2007). The shortfalls of these 3D culture systems can be addressed using a 3D perfusion bioreactor system.

Next to enhancing the mass transport in the culture system, the combination of a 3D carrier and volumetrically controlled mass transport through perfusion has the potential to guide cell fate in function of culture conditions applied. In a range between 10^{-4} Pa and 10^{-1} Pa the SS exerted by the fluid flow on the developing construct has already been shown to have an enhancing effect on both osteogenic differentiation and mineralised matrix deposition, when the fluid flow is used as an additional stimuli combined with osteogenic inductive medium (Goldstein *et al.* 2001; Bancroft *et al.* 2002; Cartmell *et al.* 2003; Gomes *et al.* 2003; Sikavitsas *et al.* 2003; Hosseinkhani *et al.* 2005; Grayson *et al.* 2008; Grayson *et al.* 2010; McCoy and O'Brien 2010; Fisher and Yeatts 2011; Grayson *et al.* 2011; Liu *et al.* 2012; McCoy *et al.* 2012; Salter *et al.* 2012). However, when the bioreactor system is intended to be used for a cell population expansion rather than the development of TE constructs containing differentiated cells, the maintenance of the progenitor phenotype is essential. Although the use of different perfusion regimes such as the use of intermittent shear stress in normal growth medium affects the behaviour of bone marrow derived Mesenchymal stem cells (MSCs) (Kim and Ma 2012), the expansion of a Mesenchymal progenitor cell population in the presence of SS with maintenance of its phenotype has proven to be possible (Scherberich *et al.* 2007). Also substrate specific interactions have the potential to trigger specific cell responses to external stimuli (Grayson *et al.* 2011), explaining the large variation in specific cell responses to SS reported in literature (McCoy and O'Brien 2010; Fisher and Yeatts 2011). Therefore, it is required to determine the effect

of a bioreactor culture on the proliferation and differentiation of a targeted cell population for specific combinations of SS and carrier material and structure.

Human periosteal derived cells (hPDCs) obtained from periost biopsies contain osteochondro-progenitor cell populations (De Bari *et al.* 2006; Eyckmans and Luyten 2006; Marolt *et al.* 2010). Their multi-lineage differentiation potential, phenotypical stability, high proliferation and accessibility make these cells a suitable cell source for bone tissue engineering (Hutmacher and Sittinger 2003; De Bari *et al.* 2006; Eyckmans and Luyten 2006; Agata *et al.* 2007; Ringe *et al.* 2008; Marolt *et al.* 2010). Several studies have already demonstrated the osteoinductive potential of these cells when implanted *in vivo* (Agata *et al.* 2007; Marechal *et al.* 2008; Roberts *et al.* 2011), and they are further being used for the development of tissue engineered bone products (Chai *et al.* 2012a; van Gastel *et al.* 2012a; van Gastel *et al.* 2012b). The use of periosteal derived cells in bioreactor systems and concomitantly the effect of such a system on the osteogenic differentiation of this cell population, is still very limited (Matziolis *et al.* 2006; Papantoniou *et al.* 2013a).

In order to determine the potential of using a perfusion bioreactor system for the expansion of this progenitor cell population, the goal of this study was to determine the influence of perfusion on the *in vitro* proliferation, differentiation and matrix formation of hPDCs in the absence of differentiation inducing medium. hPDCs were cultured on inert Ti6Al4V porous scaffolds at different flow rates corresponding to the range of SS values used in literature and proliferation was evaluated in function of the applied SS based on DNA content. Thereafter the influence of two levels of SS, reported to respectively have a proliferation enhancing or osteogenic inductive effect, on the cell behaviour was determined and compared with static 3D culture. Real time PCR (RT-

PCR) was employed to analyse gene expression in combination with the analysis of the proliferation. Contrast enhanced nanofocus X-ray computed tomography (CE-nanoCT) was employed in combination with Live/Dead staining to visualise and quantify the 3D dynamics of cell growth and extracellular matrix deposition.

2. Materials and methods

2.1 Ti6Al4V Scaffolds

Regular, 3D additive manufactured Ti6Al4V scaffolds (Ø = 6 mm, h = 6 mm) were produced in-house using selective laser melting based on a diamond shaped unit cell (Van Bael *et al.* 2011; Pyka *et al.* 2012) (Fig. 1.A). The total volume of the scaffolds was 166 ± 3 mm^3, the available volume 130 ± 5 mm^3 and the available surface 7.5 ± 0.6 mm^2 as determined with nanoCT (Kerckhofs *et al.* 2013). Prior to use, scaffolds were ultrasonically cleaned for 10 min consecutively with acetone, ethanol and distilled water. Subsequently they received an alkali treatment with 5M sodium hydroxide (Sigma-Aldrich) at 60°C for 24 hours, were rinsed with distilled water, and finally sterilised in a steam autoclave. Prior to cell seeding, all scaffolds were pre-wetted by vacuum impregnation in cell culture medium for 2 h in a humidified incubator at 37°C, and dried overnight in a non-humidified incubator (Impens *et al.* 2010; Papantoniou *et al.* 2013a; Papantoniou *et al.* 2013b; Zhou *et al.* 2013).

2.2 Fluid flow modelling

In order to determine the SS correlated with the volumetric perfusion velocity and hence select a relevant range of flow rates, fluid flow modelling using computational fluid dynamics (CFD) was used as described by Truscello *et al.*, 2012. Due to the symmetrical design of the scaffold the calculations were limited to one geometrical unit

cell. A 3D geometrical model of a scaffold unit cell was created and meshed in the ACIS-based solid modeller Gambit 2.2 (Fluent). The mesh was refined until the solution was stable (mesh independent) and contained 750 000 elements which were sized to 30 μm^3. To determine velocity fields and the related SS in the scaffold the finite volume code Fluent 6.3 (Fluent) was used. The culture medium was considered to be an incompressible and homogeneous Newtonian fluid with properties equal to water (viscosity: 10^{-3} Pa s, density: 10^3 kg/m^3, temperature: 37 °C). Since the Reynolds number was lower than 1 the correlation between the flow rate and the SS was linear. Therefore the correlation between the flow rate and the SS was determined for one flow rate and thereafter extrapolated to the range of interest. A constant velocity of 2.36 mm/s was assigned to the inlet, corresponding to a volumetric flow rate of 4 ml/min. No-slip conditions were applied to the walls of the scaffolds, symmetry conditions to the lateral surfaces and a zero gauge pressure was set at the outlet. The flow problem was described with steady-state Navier-Stokes equations.

2.3 hPDC culture

hPDCs were isolated from periosteal biopsies of different donors as described previously (Eyckmans and Luyten 2006). This procedure was approved by the ethics committee for Human Medical Research (KU Leuven) and with patient informed consent. hPDCs were expanded in Dulbecco's modified Eagle's medium with high-glucose (Invitrogen) containing 10% foetal bovine serum (Gibco), 1% sodium pyruvate (Invitrogen) and 1% antibiotic–antimycotic (100 units/mL penicillin, 100 mg/mL streptomycin, and 0.25mg/mL amphotericin B; Invitrogen). The cells were seeded at 5 700 cells/cm^2 and passaged at 80 % – 90 % confluence. Prior to the 3D culture experiments cells were harvested using Triple Express (Invitrogen) and drop-seeded by

a single drop onto the scaffolds at a density of 200 000 cells per 60µl drop as performed in earlier studies (Papantoniou *et al.* 2013a; Papantoniou *et al.* 2013b; Zhou *et al.* 2013). 45 min after seeding 60 µl culture medium was added and 135 min later the medium volume was topped up to 1 ml. Scaffold-cell constructs (further mentioned as constructs) were incubated overnight in standard culture conditions (37°C, 5% CO_2, 95% relative humidity). Since the seeding process resulted in homogenous and reproducible seeding efficiencies in earlier experiments (~60%) this was not assessed separately in this work (Papantoniou *et al.* 2013a; Papantoniou *et al.* 2013b). This seeding procedure resulted in an initial cell density of 17 100 cells/cm² or $7*10^5$ cells/cm³.

For the initial flow rate screening 5 different values (0.04, 0.25, 1, 4 and 6 ml/min) were applied, corresponding with a SS range of $5.6*10^{-4}$ Pa to $8.4*10^{-2}$ Pa, thereby covering the range of SS reported in literature (McCoy and O'Brien 2010). 30 scaffolds were seeded as described before (5 scaffolds per flow rate and 5 as static control). After the overnight static incubation, the constructs were transferred to a 12 well plate containing 3ml culture medium/well for static culture or to an in-house developed bioreactor system. This system contained in total 13 ml of culture medium for perfusion culture of which 3 ml was located in the circuit and the remaining 10 ml in the medium reservoir. Medium was refreshed every two days either by attaching a new medium reservoir containing 10 ml of fresh culture medium or by manually replacing the 3 ml of culture medium for the static constructs. Continuous perfusion was applied for a total duration of 21 days.(Papantoniou *et al.* 2013a; Papantoniou *et al.* 2013b; Zhou *et al.* 2013).

For the time point experiment 54 scaffolds were seeded and afterwards divided in 3 groups for static culture and perfusion at low and high flow rate (0.04 ml/min and 4 ml/min) corresponding with SS values reported to have a proliferation of differentiation

enhancing effect in different systems (McCoy and O'Brien 2010). Samples were taken at 14, 21 and 28 days. Time points were chosen to allow for the different stages of possible osteogenic differentiation and matrix deposition to occur.

As a positive control for mineralisation constructs were cultured for 21 days at the high flow rate using a bioinstructive medium based on normal growth medium with the addition of 6 mM Ca^{2+}, 4 mM P_i and 0.05 ng/ml ascorbic acid (Chai *et al.* 2012b; Papantoniou *et al.* 2013a).

2.4 DNA measurement

The DNA content was determined using a highly quantitative and selective DNA assay (Quant-iT^{TM} dsDNA HS kit, Invitrogen). The methods used were developed and optimised for combined DNA measurement and RNA extraction from 3D constructs (Chai *et al.* 2012a; Chen *et al.* 2012; Papantoniou *et al.* 2013a). The constructs were rinsed with PBS and lysed in 350 µl RLT lysis buffer (Qiagen) supplemented with 3.5 µl β-mercaptoethanol after which the lysed samples were vortexed for 60 s and stored at -80°C. Prior to analysis, the samples were thawed at room temperature and spun down for 1 min at 13 000 rpm. 10 µl of the sample was diluted in 90 µl milliQ water after which the DNA content was quantified with a Qubit® Fluorometer (Invitrogen) as described by Chen *et al.*, 2012.

2.5 Quantitative PCR

For the time point experiment, RNA was extracted from 4 random, representative constructs for each culturing condition and time point using the RNeasy mini kit (Qiagen) and quantified using a Nanodrop ND-1000 spectrophotometer (Thermo Scientific). Complementary DNA was synthesised using the RevertAid H Minus First Strand complementary DNA synthesis kit (Fermentas). Sybr green quantitative

polymerase chain reaction was performed for different key osteogenic and chondrogenic markers (Sox9, Col1, RunX2, OCN, OPN, OSX and BSP (Chai *et al.* 2012a)) and compared to HPRT (HPRT-F, 5'-TGAGGATTTGGAAAGGGTGT-3'; HPRT-R, 5'-GAGCACACAGAGGGCTACAA-3'). The PCR reaction was cycled in a Rotor-Gene sequence detector (Qiagen) as follows: 95 °C for 3 min, 40 cycles of 95 °C for 3 s and 60 °C for 60 s. Differences in gene expression were determined relatively in comparison to HPRT and shown as $2^{-\Delta CT}$.

For the constructs cultured with or without bioinstructive mineralisation medium for 21 days the expression of Sox9, OCN, OPN and OSX was determined. Differences in gene expression were shown relative to HPRT expression and to the static control ($2^{-\Delta\Delta CT}$).

2.6 Contrast-enhanced nanofocus computed tomography (CE-nanoCT)

CE-nanoCT was performed on two random, representative constructs for each time point and culture condition as described earlier (Papantoniou *et al.* 2013b). The constructs were fixed in 4% paraformaldehyde (Sigma) for two hours and stored in PBS prior to analysis. Hexabrix® 320 (Guerbet) was used as a contrast agent to visualise the neo-tissue formed in the construct (Papantoniou *et al.* 2013b). As the Hexabrix® is an equilibrium contrast agent it will equally infiltrate all non-negatively charged tissues and thereby enable the visualisation of the radio-transparent neo-tissue in the opaque Ti6Al4V structure.

A Phoenix NanoTom S (GE Measurement and Control Solutions) with a 180 kV/15 W high-performance nanofocus X-ray tube was used to perform the CE-nanoCT. A tungsten target was operated at a voltage of 90 kV and a current of 170 µA. An aluminium and copper filter, both 1 mm thick, were used to reduce beam hardening and metal artefacts. The exposure time was 500 ms, a frame averaging of 1 and image skip

of 0 were applied, resulting in a scanning time of 20 min. The reconstructed images had an isotropic voxel size of 3.75 µm.

2.7 3D visualisation, image processing and analysis

CTAn (Bruker micro-CT) was used for image processing as described by Papantoniou *et al*., 2013b. Briefly, the neo-tissue was separated from the background noise and the scaffold using a 2-level Otsu thresholding method (Otsu 1979), resulting in a greyscale image containing 3 fractions, respectively background, neo-tissue and scaffold material. To analyse the volume of the Ti6Al4V scaffolds the resulting greyscale dataset was thresholded to obtain binary images representing the scaffold. In order to subsequently reduce the influence of the partial volume effect, edge effects and metallic artefacts introduced by the presence of the Ti6Al4V scaffold while analysing the neo-tissue volume, the binarised images for the scaffold were dilatated by two voxels and subtracted from the region of interest for further analysis. The neo-tissue fraction within the new region of interest was then binarised and the noise was removed by removing black speckles smaller than 500 voxels and white speckles smaller than 2 000 voxels. To solidify the resulting structure, a ’closing’ operation (~ 2 voxels) was performed on the resulting images, providing the images used for the 3D analysis of the neo-tissue volume.

2.8 Live/Dead assay

A Live/Dead viability/cytotoxicity kit (Invitrogen) was used to evaluate qualitatively cell viability and cell distribution by optical microscopy. For each culture condition two random, representative constructs were imaged of which one was subsequently used for CE-nanoCT and one for DNA measurement and RNA extraction. Constructs were rinsed with 1 ml PBS after which they were incubated in the staining solution (0.5 µl of

a 4mM Calcein AM in anhydrous DMSO solution and 2 µl of a 2mM Ethidium Homodimer in DMSO/H_20 (1:4, v:v) in 1 ml PBS) for 20 min in normal cell culture conditions. The constructs were imaged using a Leica M165 FC microscope.

2.9 Alizarin red staining

Constructs cultured for 21 days with normal growth medium or bioinstructive medium were fixed in 4% paraformaldehyde and stored in PBS prior to staining. Staining was performed with a 2% Alizarin Red S (Sigma) solution in water (pH 4.2) for 1 hour at room temperature during continuous gentle agitation. Samples were subsequently rinsed with demineralised water until no additional staining was removed from the constructs after which they were imaged using a stereo microscope (Leica M165 FC).

2.10 Statistical analysis

Student t-test was performed to analyse significant differences between groups using Statistica 7 (Statsoft). A p-value < 0.05 was considered significant.

3. Results

3.1 Shear stress range

CFD was used to determine the initial SS which the fluid exerted on the constructs in order to compare our results with other reports (Grayson *et al.* 2011; Kim and Ma 2012). Since the scaffold design consists of a repetition of a regularly shaped diamond unit cell (Fig. 1.A), the calculations were performed for only one unit cell (Truscello *et al.* 2012). Figs. 1.B-C show a 3D visualisation of the SS on a scaffold unit cell and the corresponding histogram of the relative SS distribution within the unit cell. Fig. 1.D shows the initial average CFD-calculated SS based on the experimentally used flow rates. The obtained distribution could be extrapolated for the other flow rates used since fluid flow remained laminar in the used range.

3.2 Proliferation

The use of different flow rates did not significantly influence the DNA content of the constructs after 21 days of dynamic culture in growth medium (Fig. 2.A). However, analysis of all perfused constructs cultured for 21 days at different flow rates showed that the DNA content of the constructs cultured in perfusion was on average 2.75 ± 0.27 fold increased in comparison with the static control. To get a better understanding of the time-dependent influence on hPDC proliferation of a constant volumetric flow rate in combination with a morphological changing matrix, which resulted in a time dependent increase in SS, the 0.04 ml/min and 4 ml/min flow rate conditions were selected and compared to the static culture for 14, 21 and 28 days. For all time-points the perfused conditions showed a significant increased DNA content in comparison to the static control. However, the static control as well as the perfused conditions did not show any significant time dependent changes from 14 up to 28 days (Fig. 2.B), although an increasing trend was still observed for the perfused constructs.

Based on our in-house 2D hPDC expansion database an average cell expansion of 2.9 ± 0.65 was determined in comparison to the initial cell density for a 7 day expansion period or 8.4 ± 2.6 in 14 day when cells are replated according to standardised cell expansion protocols (n=20).

3.3 Live/Dead staining

Cell distribution at the periphery of the constructs was visualised using the Live-Dead viability/cytotoxicity kit (Fig. 3.). For both the statically cultured and the 0.04 ml/min perfused samples the construct was fully covered with cells after 21 days of culture. For the high flow rate (4 ml/min) the cell coverage of the outer surfaces did not seem to increase over time for the imaged time points. A clearly less dense coverage of the

surface was observed in comparison with the two previously described conditions. There were no significant amounts of dead cells observed in any of the examined conditions.

3.4 3D matrix image analysis by CE-nanoCT

CE-nanoCT using Hexabrix® as contrast agents was used to visualise and quantify in 3D the neo-tissue formed in the constructs. Fig. 4 shows axial 2D cross-sections representative for the entire construct for 0.04 and 4 ml/min as well as the static control for different time points. In the raw images (left 3 columns) the white zones represent the scaffold structure, while the delineated grey features represent the neo-tissue in the constructs. The binarised images (right) show the quantified neo-tissue fraction in white. In correspondence with the Live/Dead staining shown in Fig. 3., the outer surface of the statically cultured constructs was nearly completely covered with cell-matrix after 14 days, which is visible as a thin line with a lighter shade of grey on the images in Fig. 4 as indicated with the arrows. Increasing the static culture duration did not result in a significant increase in cell-matrix volume for these constructs. The perfusion cultured constructs showed that the morphology of the cell-matrix formed was influenced by the culture condition. Instead of forming a cell sheet on the outer edges of the construct as was the case for the static control, cell-matrix was formed throughout the entire scaffold resulting in a much denser and more filled construct as was also observed by DNA analysis (Fig. 2.B). In both the 0.04 ml/min and 4 ml/min perfused culture the Hexabrix® based images showed that the cell-matrix was gradually filling up the available space in the construct.

As reported earlier, the amount of cell-matrix present in the statically cultured constructs was too low to be quantified (Papantoniou *et al.* 2013b). As shown in Figure

4 the neo-tissue developed in these constructs was fibrous in appearance and was only located in thin strands (average diameter of about 5 µm as determined with DataViewer, Bruker MicroCT) at the outer edges of the constructs. Although most of these structures can be visually discriminated in the CE-nanoCT images, the limited contrast difference between the stained neo-tissue and the background did not allow to accurately segment both from each other, resulting in an erroneous quantification of the neo-tissue volume. Therefore, quantitative analysis of the cell-matrix volume was performed only on the perfused constructs. In Fig.5., the relative filling volume, determined using Hexabrix® as a contrast agent, was normalised to DNA content. For the high flow rate, a stronger increase after 21 days of culture was observed compared to the low flow rate where this increase was only observed after 28 days indicating a difference in matrix deposition kinetics. At the final time-point however, no differences in deposited matrix per cell was present.

3.5 Gene expression analysis

Finally gene expression analysis was performed to assess the influence of the different culture conditions on cell differentiation (Fig 6.). For the statically cultured constructs a significant down regulation of the Col1 expression was observed in function of time. The 14 and 21 day expression of Col1 in the perfused conditions was also down-regulated in comparison to the static constructs but this difference was no longer present at the 28 day time point. For RunX2 the expression remained stable in function of time for the static constructs and no differences were observed between the static and perfused conditions. For the low flow rate a significant increase was observed between day 14 and 28. For the high flow rate this increase was observed at the 21 day time point, although it was no longer present at the final day 28 time point. In the case of

OCN no significant differences were observed between the static controls and both perfused conditions. At day 14 a higher expression was observed for the low flow rate in comparison to the high flow rate but this difference was no longer observed at later time points. Except for the low flow rate at day 14 no differences were observed in OPN expression between the static control and the perfused conditions. Although a time dependent increase was observed for the low flow rate, OPN expression was significantly higher for the high flow rate in comparison to the low flow rate. BSP showed a time-dependent increase in both perfused conditions resulting in a significantly higher expression in comparison to the static control at day 28. No significant differences between the perfused conditions were observed. Sox9 expression decreased significantly over time in the static control. In both perfused conditions Sox9 expression was significantly lower at day 14 and 21 but this difference was no longer observed at day 28. OSX expression showed a time dependent decrease in the static control. Except at day 14 no differences were present between the static control and the low flow rate condition. The high flow rate showed a significantly higher expression in comparison to the low flow rate (all time points) and to the static control (after 21 and 28 days).

4. Discussion

Perfusion bioreactor systems show great promise as a tool for automated 3D cell expansion and their use will be essential for the clinical implementation of current tissue engineering and regenerative medicine strategies (Martin *et al.* 2010; Fisher and Yeatts 2011; Salter *et al.* 2012). Therefore, it is imperative to understand the influence of the process environment on the behaviour and properties of the cell populations expanded in these systems and define suitable operating conditions which support cell expansion

while maintaining a progenitor cell phenotype. The present study used hPDCs seeded on a Ti6Al4V scaffold in a perfusion bioreactor system to determine its potential for cell expansion by evaluating the influence of flow-induced SS on the proliferation, differentiation and extracellular cell-matrix deposition in the absence of additional differentiation-inducing stimuli such as osteogenic inductive medium.

3D perfusion bioreactor culture has been extensively used for the production of bone TE constructs and has shown to significantly increase proliferation, differentiation and mineralised matrix deposition in comparison to static controls (McCoy and O'Brien 2010; Fisher and Yeatts 2011). Additionaly, SS dependent increases in proliferation and mineralisation have been reported for MSCs in combination with osteogenic medium (Bancroft *et al.* 2002; Cartmell *et al.* 2003; Sikavitsas *et al.* 2003; McCoy and O'Brien 2010). Additionally, the use of intermittent shear stresses exerted on the a construct developing in normal growth medium resulted in the significant induction of an osteogenic phenotype in comparison to the continuous shear conditions, although no comparison with a static control was made here (Liu *et al.* 2012). In correspondence with this literature data, our work showed that perfusion significantly increased the cell number on the Ti6Al4V scaffolds in comparison to the static control (Fig. 2.A), as both dynamic conditions resulted in a significant increase in DNA content in comparison to the static control for all time points. The enhanced mass transport present in a perfusion setup in comparison to the static setup will provide an optimal nutrient supply to the entire construct, thereby enabling all the cells in the construct to proliferate under more optimal conditions. This was confirmed with the CE-nanoCT which shows that the developed neo-tissue is only present at the outer edges of the statically cultured constructs while in both perfused conditions the neo-tissue is deposited uniformly

throughout the entire construct. As the use of a higher flow rate did not significantly improve the nutrient supply to the developing constructs, the absence of correlated changes in proliferation could be explained, as also reported earlier for similar systems using osteogenic medium supplements (Sikavitsas *et al.* 2003; Dai *et al.* 2009; Grayson *et al.* 2011).

An average cell density increase of 3.6 ± 0.6 times, with respect to the static constructs or an 8.4 ± 1.7 fold increase in relation to the initial cell density were observed after 28 days (Figure 2.B). These expansion rates were not significantly different from those observed in the standard 2D culture at the 14 day time point for the high flow rate (8.4 ± 2.6 for 2D vs 7 ± 1.2 in the perfusion system), without the need for replating. For later time points the proliferation rate, based on the DNA measurement, in the 3D perfusion bioreactor setup decreased, due to the gradual filling and closing of the open spaces in the construct as shown in Fig. 4. In 2D culture systems a decrease in proliferation is also observed when cells are not replated prior to confluence, but for 2D static culture systems this phenomenon already occurs after 8 to 10 days resulting in an average cell expansion of 4 to 5 times. This shows that the perfusion bioreactor system performs at least as efficient as a standard 2D sub-culture system with regard to cell expansion, but not requiring manual intermediate trypsinisation and replating steps.

Besides conventional, manual, 2D cell expansion, the use of micro carriers is often mentioned to be a promising technique for automated cell expansion despite the absence of a real 3D environment (dos Santos *et al.* 2011; Hewitt *et al.* 2011; Goh *et al.* 2013). In these systems 7 to 20 fold increases in cell number have been reported after already 7 days of cell expansion resulting in significantly higher expansion rates in comparison to the 3D perfusion bioreactor system used for this work. However, the maximal cell

density that could be obtained in micro-carrier based expansion systems is on average between $2*10^5$ and $8*10^5$ cells/cm³ (dos Santos *et al.* 2011; Hewitt *et al.* 2011; Goh *et al.* 2013) while, based on the DNA content and assuming an average of 8.9 pg DNA/cell as reported earlier (Zhou *et al.* 2013), the 3D perfusion system used in this work reached a cell density of 5 to $6*10^6$ cells/cm³. This demonstrates that a higher cell number per volume unit can be obtained, thereby indicating their high cell expansion potential per volumetric unit. Additionally, current protocols for the 3D perfusion bioreactor system have not been optimised yet for cell expansion. Reducing the initial cell seeding density in the system from $7*10^5$ cells/cm³ or 17 100 cells/cm² to the densities which are currently used for micro carrier expansion (10 to 20 fold lower (Hewitt *et al.* 2011)) could further increase the yield of the 3D perfusion bioreactor culture.

Live/dead staining of the constructs showed that no the flow rate had no significant influence on the cell viability in the outer layers of the formed neo-tissue (Fig.3). The differences in DNA content between static and dynamically cultured constructs could not be visually confirmed. However, microscope-based live/dead staining is a line-of-sight visualisation technique, allowing only observation of the peripheral part of the scaffold, hence a novel imaging technique, CE-nanoCT was used in order to monitor cell growth and provide quantitative volumetric information regarding cell and extracellular matrix distribution throughout the entire volume of the scaffold (Fig. 4)(Papantoniou *et al.* 2013b). CE-nanoCT images showed a time dependent 3D filling of the scaffold void volume. For the static constructs cell-matrix was only situated on the outer edges of the construct as reported by other groups using destructive 2D based techniques such as histology (Ishaug *et al.* 1997; Bancroft *et al.* 2002; Sikavitsas *et al.*

2003). In function of time not only was more cell-matrix deposited but also the amount of cell-matrix deposited per cell, as calculated based on the CE-nanoCT based images and the measured DNA content, increased for both flow rates as observed by the Hexabrix® based images (Fig. 4, Fig. 5. As higher SS has been reported to result in increased matrix deposition (Jaasma *et al.* 2008; Grayson *et al.* 2011), the increase in SS present in the developing constructs due to the filling of the available volume could explain the observed increase in matrix deposition per cell. Despite the difference in matrix deposition kinetics no differences in matrix deposition were observed for the different flow rates at the final timepoint.

In this work initial SS values exerted on the developing constructs, as determined by CFD, ranged between $5.59*10^{-4}$ and $8.38*10^{-2}$ Pa. Although in this range, enhanced osteogenic differentiation and collagen production has been previously reported for MSCs in combination with osteogenic medium (McCoy and O'Brien 2010) its influence in normal growth medium is not known. The SS values determined using CFD were based on the empty Ti6Al4V scaffold geometry. However, as observed by the experimental data, cell and matrix growth gradually filled up the internal volume of the Ti6Al4V scaffold, thereby significantly altering the flow environment. The increase in cell-matrix volume will reduce the volume available for the fluid to flow through, thereby increasing the flow rate of the medium and the correlated SS. Calculated SS values will therefore more closely represent those SS values that hPDCs will experience during the initial period of the bioreactor culture and serve mainly as a reference for comparison with literature data in which a similar approach was used (Bancroft *et al.* 2002; Sikavitsas *et al.* 2003; Kim and Ma 2012; Liu *et al.* 2012). In future work the neo-tissue filling determined via CE-nanoCT as function of culture duration may be

used as input for CFD modeling to obtain dynamic SS information to which the cells are actually exposed during the expansion process.

To further assess the influence of flow rate on the hPDCs the expression of a range of of genes was analysed to determine cell commitment towards a specific lineage (Fig 6.). Results showed that Sox9 was significantly down-regulated for both perfusion conditions at day 14 and 21 in comparison to the static control, but that this was no longer the case at day 28 due to the gradual decrease observed in the static control. Sox9 expression was already shown to be increased in a perfusion system in chondrogenic medium (Tigli *et al.* 2011) but, in correspondence with our findings, there were no reports of increased chondrogenic differentiation in the absence of biochemical inducers in a perfusion system. Therefore no additional chondrogenic markers were evaluated in this work. Different osteogenic markers, such as Col1, RunX2, OPN and OCN, showed limited time-dependent changes in expression. In accordance to previously reported data (Bjerre *et al.* 2008; Kim and Ma 2012), certain flow-rate-dependent changes in expression were observed, but perfusion as such did not have a significant influence on the expression of these key osteogenic markers as no differences between the static control and the perfused conditions were present (Fig 6.). Additionally, the limited observed time dependent changes in expression of these markers are negligible in comparison to what was reported earlier for induced osteogenic differentiation for this cell type (Chai *et al.* 2011). Despite that no significant changes were observed in the expression of ECM related genes such as Col1 and OCN significant differences in the ECM deposition per cell were observed between the different conditions. The culture of cells under shear stress has earlier been shown to potentially induce changes in posttranscriptional regulation of certain ECM proteins (Bjerre et al. 2008) and

differences in the incorporation of secreted matrix proteins (Grayson et al. 2011). This indicates that SS can significantly influence the composition of the deposited neo-tissue in a 3D culture system without influencing gene expression, thus potentially explaining the differences in neo-tissue volume deposited in static versus the perfused conditions.

BSP on the other hand showed, compared to the static control, an 8-fold time-dependent increase in expression in both perfused conditions. However, as shown by Grayson *et al*, 2011 the combination of perfusion and osteogenic medium can result in a 100-fold increase in BSP expression after one week and even a 1 000-fold increase after 5 weeks of perfusion culture using MSCs (Grayson *et al.* 2011), indicating that the increase observed in our study is limited for both perfused conditions. For OSX, an important early osteogenic transcription factor (Kim and Ma 2012), a flow rate dependent increase in expression was observed. In the normal osteogenic differentiation cascade of events this increase would be preceded by an increase in RunX2, of which OCN is a downstream target, and followed by an increased expression of BSP and OCN (Lian *et al.* 2006; Franceschi *et al.* 2007; Kim and Ma 2012). This cascade of events was however not observed in the studied system. Although the expected initial increase of RunX2 in osteogenic differentiation could have occurred at an earlier time point and a subsequent increase in BSP expression was present no differences in OCN expression were detected. In the absence of the OCN increase, the increased OSX expression could be explained by cell lineage commitment rather than to full osteogenic differentiation.

This was confirmed by comparing the expression of Sox9, OCN, OPN and OSX for constructs cultured for 21 days using normal growth medium and bioinstructive mineralisation medium (Figure 7.A). Although a significant lower Sox9 expression was detected in the normal constructs after 21 days, a 100-fold stronger decrease in

expression was present in the induced constructs. For the OCN, OPN and OSX expression respectively a 12-, 90- and 6-fold increase in expression was detected for the induced constructs in comparison with the growth medium cultured. Alizarin red staining visually confirmed the presence of a mineralised matrix in the induced constructs (Figure 7.C), while this was not detected in the growth medium constructs (Figure 7.B). This further confirmed that expansion of the MSC like hPDC cell population in a perfusion bioreactor system does not result in significant osteogenic differentiation nor in an associated mineralised matrix deposition although there are indications of osteogenic lineage commitment as shown by the increased OSX and BSP expression.In conclusion, we can state that, for our experimental set-up, perfusion bioreactor culture resulted in expansion rates similar to those obtained in different validated cell expansion systems. Additionally, the system did not induce significant changes in the expression pattern of the osteogenic and chondrogenic markers analysed. Although small differences in the expression of certain markers were observed between different flow rates, these were limited in comparison to the reported increases in expression when using osteo- or chondro-inductive media in both static and perfused conditions as well as to changes in gene expression in the constructs cultured with bioinstructive mineralisation medium. Perfusion did however significantly increase cell proliferation and resulted in flow rate-dependent changes in matrix deposition kinetics. These results indicate the potential of perfusion bioreactor facilitated stem cell expansion.

Acknowledgements

MS is supported by a Ph.D. grant of the Agency for Innovation by Science and Technology (IWT/ 111457). IP is funded by the ENDEAVOUR project G.0982.11N of the Research Foundation Flanders (FWO Vlaanderen). GK acknowledges support by the European Research Council under the European Union's Seventh Framework Program (FP7/2007-2013)/ERC grant agreement n°279100. The X-ray computed tomography images have been generated on the X-ray computed tomography facilities of the Department MTM of the KU Leuven, financed by the Hercules Foundation (project AKUL 09/001: Micro-and nano-CT for the hierarchical analysis of materials) This work is part of Prometheus, the Leuven Research & Development Division of Skeletal Tissue Engineering of the KU Leuven: www.kuleuven.be/prometheus

Bibliography

Agata, H., I. Asahina, Y. Yamazaki, M. Uchida, Y. Shinohara, M. J. Honda, H. Kagami and M. Ueda 2007, Effective bone engineering with periosteum-derived cells, *Journal of Dental Research* **86**(1): 79-83.

Bancroft, G. N., V. I. Sikavitsas, J. van den Dolder, T. L. Sheffield, C. G. Ambrose, J. A. Jansen and A. G. Mikos 2002, Fluid flow increases mineralized matrix deposition in 3D perfusion culture of marrow stromal osteoblasts in a dose-dependent manner, *Proc Natl Acad Sci U S A* **99**(20): 12600-12605.

Bjerre, L., C. E. Bunger, M. Kassem and T. Mygind 2008, Flow perfusion culture of human mesenchymal stem cells on silicate-substituted tricalcium phosphate scaffolds, *Biomaterials* **29**(17): 2616-2627.

Cartmell, S. H., B. D. Porter, A. J. Garcia and R. E. Guldberg 2003, Effects of medium perfusion rate on cell-seeded three-dimensional bone constructs in vitro, *Tissue Eng* **9**(6): 1197-1203.

Chai, Y. C., S. J. Roberts, E. Desmet, G. Kerckhofs, N. van Gastel, L. Geris, G. Carmeliet, J. Schrooten and F. P. Luyten 2012a, Mechanisms of ectopic bone formation by human osteoprogenitor cells on CaP biomaterial carriers, *Biomaterials* **33**(11): 3127-3142.

Chai, Y. C., S. J. Roberts, J. Schrooten and F. P. Luyten 2011, Probing the osteoinductive effect of calcium phosphate by using an in vitro biomimetic model, *Tissue Eng Part A* **17**(7-8): 1083-1097.

Chai, Y. C., S. J. Roberts, S. Van Bael, Y. Chen, F. P. Luyten and J. Schrooten 2012b, Multi-Level Factorial Analysis of Ca2+/P-i Supplementation as Bio-Instructive Media for In Vitro Biomimetic Engineering of Three-Dimensional Osteogenic Hybrids, *Tissue Engineering Part C-Methods* **18**(2): 90-103.

Chang, J., H. Lei, Q. Liu, S. Qin, K. Ma, S. Luo, X. Zhang, W. Huang, Z. Zuo, H. Fu and Y. Xia 2012, Optimization of culture of mesenchymal stem cells: a comparison of conventional plate and microcarrier cultures, *Cell Prolif* **45**(5): 430-437.

Chen, X. D., V. Dusevich, J. Q. Feng, S. C. Manolagas and R. L. Jilka 2007, Extracellular matrix made by bone marrow cells facilitates expansion of marrow-derived mesenchymal progenitor cells and prevents their differentiation into osteoblasts, *Journal of Bone and Mineral Research* **22**(12): 1943-1956.

Chen, Y. T., M. Sonnaert, S. J. Roberts, F. P. Luyten and J. Schrooten 2012, Validation of a PicoGreen-Based DNA Quantification Integrated in an RNA Extraction Method for Two-Dimensional and Three-Dimensional Cell Cultures, *Tissue Engineering Part C-Methods* **18**(6): 444-452.

Dai, K. R., D. Q. Li, T. T. Tang and J. X. Lu 2009, Effects of Flow Shear Stress and Mass Transport on the Construction of a Large-Scale Tissue-Engineered Bone in a Perfusion Bioreactor, *Tissue Engineering Part A* **15**(10): 2773-2783.

De Bari, C., F. Dell'Accio, J. Vanlauwe, J. Eyckmans, Y. M. Khan, C. W. Archer, E. A. Jones, D. McGonagle, T. A. Mitsiadis, C. Pitzalis and F. P. Luyten 2006, Mesenchymal multipotency of adult human periosteal cells demonstrated by single-cell lineage analysis, *Arthritis and Rheumatism* **54**(4): 1209-1221.

dos Santos, F., P. Z. Andrade, G. Eibes, C. L. da Silva and J. M. Cabral 2011, Ex vivo expansion of human mesenchymal stem cells on microcarriers, *Methods Mol Biol* **698**: 189-198.

Eyckmans, J. and F. P. Luyten 2006, Species specificity of ectopic bone formation using periosteum-derived mesenchymal progenitor cells, *Tissue Eng* **12**(8): 2203-2213.

Fisher, J. P. and A. B. Yeatts 2011, Bone tissue engineering bioreactors: Dynamic culture and the influence of shear stress, *Bone* **48**(2): 171-181.

Franceschi, R. T., C. X. Ge, G. Z. Xiao, H. Roca and D. Jiang 2007, Transcriptional regulation of osteoblasts, *Skeletal Biology and Medicine, Pt A* **1116**: 196-207.

Goh, T. K., Z. Y. Zhang, A. K. Chen, S. Reuveny, M. Choolani, J. K. Chan and S. K. Oh 2013, Microcarrier culture for efficient expansion and osteogenic differentiation of human fetal mesenchymal stem cells, *Biores Open Access* **2**(2): 84-97.

Goldstein, A. S., T. M. Juarez, C. D. Helmke, M. C. Gustin and A. G. Mikos 2001, Effect of convection on osteoblastic cell growth and function in biodegradable polymer foam scaffolds, *Biomaterials* **22**(11): 1279-1288.

Gomes, M. E., V. I. Sikavitsas, E. Behravesh, R. L. Reis and A. G. Mikos 2003, Effect of flow perfusion on the osteogenic differentiation of bone marrow stromal cells cultured on starch-based three-dimensional scaffolds, *Journal of Biomedical Materials Research Part A* **67A**(1): 87-95.

Grayson, W. L., S. Bhumiratana, C. Cannizzaro, P. H. Chao, D. P. Lennon, A. I. Caplan and G. Vunjak-Novakovic 2008, Effects of initial seeding density and fluid perfusion rate on formation of tissue-engineered bone, *Tissue Eng Part A* **14**(11): 1809-1820.

Grayson, W. L., M. Frohlich, K. Yeager, S. Bhumiratana, M. E. Chan, C. Cannizzaro, L. Q. Wan, X. S. Liu, X. E. Guo and G. Vunjak-Novakovic 2010, Engineering anatomically shaped human bone grafts, *Proceedings of the National Academy of Sciences of the United States of America* **107**(8): 3299-3304.

Grayson, W. L., T. Ma and B. Bunnell 2004, Human mesenchymal stem cells tissue development in 3D PET matrices, *Biotechnol Prog* **20**(3): 905-912.

Grayson, W. L., D. Marolt, S. Bhumiratana, M. Frohlich, X. E. Guo and G. Vunjak-Novakovic 2011, Optimizing the Medium Perfusion Rate in Bone Tissue Engineering Bioreactors, *Biotechnology and Bioengineering* **108**(5): 1159-1170.

Haycock, J. W. 2011, 3D cell culture: a review of current approaches and techniques, *Methods Mol Biol* **695**: 1-15.

Hewitt, C. J., K. Lee, A. W. Nienow, R. J. Thomas, M. Smith and C. R. Thomas 2011, Expansion of human mesenchymal stem cells on microcarriers, *Biotechnology Letters* **33**(11): 2325-2335.

Hosseinkhani, H., Y. Inatsugu, Y. Hiraoka, S. Inoue and Y. Tabata 2005, Perfusion culture enhances osteogenic differentiation of rat mesenchymal stem cells in collagen sponge reinforced with poly(glycolic acid) fiber, *Tissue Engineering* **11**(9-10): 1476-1488.

Hutmacher, D. W. and M. Sittinger 2003, Periosteal cells in bone tissue engineering, *Tissue Engineering* **9**: S45-S64.

Impens, S., Y. Chen, S. Mullens, F. Luyten and J. Schrooten 2010, Controlled Cell-Seeding Methodologies: A First Step Toward Clinically Relevant Bone Tissue Engineering Strategies, *Tissue Eng Part C Methods* **16**(6): 1575-1583.

Ishaug, S. L., G. M. Crane, M. J. Miller, A. W. Yasko, M. J. Yaszemski and A. G. Mikos 1997, Bone formation by three-dimensional stromal osteoblast culture in biodegradable polymer scaffolds, *J Biomed Mater Res* **36**(1): 17-28.

Jaasma, M. J., N. A. Plunkett and F. J. O'Brien 2008, Design and validation of a dynamic flow perfusion bioreactor for use with compliant tissue engineering scaffolds, *Journal of Biotechnology* **133**(4): 490-496.

Jakob, M., F. Saxer, C. Scotti, S. Schreiner, P. Studer, A. Scherberich, M. Heberer and I. Martin 2012, Perspective on the Evolution of Cell-Based Bone Tissue Engineering Strategies, *European Surgical Research* **49**(1): 1-7.

Jung, S., K. M. Panchalingam, R. D. Wuerth, L. Rosenberg and L. A. Behie 2012, Large-scale production of human mesenchymal stem cells for clinical applications, *Biotechnol Appl Biochem* **59**(2): 106-120.

Kerckhofs, G., G. Pyka, M. Moesen, S. Van Bael, J. Schrooten and M. Wevers 2013, High-Resolution Microfocus X-Ray Computed Tomography for 3D Surface Roughness Measurements of Additive Manufactured Porous Materials, *Advanced Engineering Materials* **15**(3): 153-158.

Kim, J. and T. Ma 2012, Perfusion regulation of hMSC microenvironment and osteogenic differentiation in 3D scaffold, *Biotechnol Bioeng* **109**(1): 252-261.

Lian, J. B., G. S. Stein, A. Javed, A. J. van Wijnen, J. L. Stein, M. Montecino, M. Q. Hassan, T. Gaur, C. J. Lengner and D. W. Young 2006, Networks and hubs for the transcriptional control of osteoblastogenesis, *Reviews in Endocrine & Metabolic Disorders* **7**(1-2): 1-16.

Liu, L., B. Yu, J. Chen, Z. Tang, C. Zong, D. Shen, Q. Zheng, X. Tong, C. Gao and J. Wang 2012, Different effects of intermittent and continuous fluid shear stresses on osteogenic differentiation of human mesenchymal stem cells, *Biomech Model Mechanobiol* **11**(3-4): 391-401.

Marechal, M., J. Eyckmans, J. Schrooten, E. Schepers, F. P. Luyten and D. van Steenberghe 2008, Bone augmentation with autologous periosteal cells and two different calcium

phosphate scaffolds under an occlusive titanium barrier: An experimental study in rabbits, *Journal of Periodontology* **79**(5): 896-904.

Marolt, D., M. Knezevic and G. V. Novakovic 2010, Bone tissue engineering with human stem cells, *Stem Cell Research & Therapy* **1**(2): 1-10.

Martin, I., H. Baldomero, C. Bocelli-Tyndall, J. Passweg, D. Saris and A. Tyndall 2012, The Survey on Cellular and Engineered Tissue Therapies in Europe in 2010, *Tissue Engineering Part A* **18**(21-22): 2268-2279.

Martin, I., H. Baldomero, C. Bocelli-Tyndall, I. Slaper-Cortenbach, J. Passweg and A. Tyndall 2011, The survey on cellular and engineered tissue therapies in europe in 2009, *Tissue Eng Part A* **17**(17-18): 2221-2230.

Martin, I., S. A. Riboldi and D. Wendt 2010, 'Bioreactor Systems in Regenerative Medicine' in *Advances in Regenerative Medicine: Role of Nanotechnology, and Engineering Principles*, Springer Science+Business Media, Dordrecht, The Netherlands, 95-113.

Martin, I., D. Wendt and M. Heberer 2004, The role of bioreactors in tissue engineering, *Trends in Biotechnology* **22**(2): 80-86.

Matziolis, G., J. Tuischer, G. Kasper, M. Thompson, B. Bartmeyer, D. Krocker, C. Perka and G. Duda 2006, Simulation of cell differentiation in fracture healing: Mechanically loaded composite scaffolds in a novel bioreactor system, *Tissue Engineering* **12**(1): 201-208.

McCoy, R. J., C. Jungreuthmayer and F. J. O'Brien 2012, Influence of flow rate and scaffold pore size on cell behavior during mechanical stimulation in a flow perfusion bioreactor, *Biotechnol Bioeng* **109**(6): 1583-1594.

McCoy, R. J. and F. J. O'Brien 2010, Influence of shear stress in perfusion bioreactor cultures for the development of three-dimensional bone tissue constructs: a review, *Tissue Eng Part B Rev* **16**(6): 587-601.

Otsu, N. 1979, Threshold Selection Method from Gray-Level Histograms, *Ieee Transactions on Systems Man and Cybernetics* **9**(1): 62-66.

Papantoniou, I., Y. C. Chai, F. P. Luyten and J. Schrooten 2013a, Process quality engineering for bioreactor-driven manufacturing of tissue engineered constructs for bone regeneration, *Tissue Eng Part C Methods* **19**(8): 596-609.

Papantoniou, I., M. Sonnaert, L. Geris, F. P. Luyten, J. Schrooten and G. Kerckhofs 2013b, Three dimensional characterization of tissue-engineered constructs by contrast enhanced nanofocus computed tomography, *Tissue Eng Part C Methods*.

Pyka, G., A. Burakowski, G. Kerckhofs, M. Moesen, S. Van Bael, J. Schrooten and M. Wevers 2012, Surface Modification of Ti6Al4V Open Porous Structures Produced by Additive Manufacturing, *Advanced Engineering Materials* **14**(6): 363-370.

Ringe, J., I. Leinhase, S. Stich, A. Loch, K. Neumann, A. Haisch, T. Haupl, R. Manz, C. Kaps and M. Sittinger 2008, Human mastoid periosteum-derived stem cells: promising candidates for skeletal tissue engineering, *J Tissue Eng Regen Med* **2**(2-3): 136-146.

Roberts, S. J., L. Geris, G. Kerckhofs, E. Desmet, J. Schrooten and F. P. Luyten 2011, The combined bone forming capacity of human periosteal derived cells and calcium phosphates, *Biomaterials* **32**(19): 4393-4405.

Rodrigues, C. A. V., T. G. Fernandes, M. M. Diogo, C. L. da Silva and J. M. S. Cabral 2011, Stem cell cultivation in bioreactors, *Biotechnology Advances* **29**(6): 815-829.

Salter, E., B. Goh, B. Hung, D. Hutton, N. Ghone and W. L. Grayson 2012, Bone Tissue Engineering Bioreactors: A Role in the Clinic?, *Tissue Eng Part B Rev* **18**(1): 62-75.

Scherberich, A., R. Galli, C. Jaquiery, J. Farhadi and I. Martin 2007, Three-dimensional perfusion culture of human adipose tissue-derived endothelial and osteoblastic progenitors generates osteogenic constructs with intrinsic vascularization capacity, *Stem Cells* **25**(7): 1823-1829.

Sikavitsas, V. I., G. N. Bancroft, H. L. Holtorf, J. A. Jansen and A. G. Mikos 2003, Mineralized matrix deposition by marrow stromal osteoblasts in 3D perfusion culture increases with increasing fluid shear forces, *Proc Natl Acad Sci U S A* **100**(25): 14683-14688.

Tigli, R. S., C. Cannizaro, M. Gumusderelioglu and D. L. Kaplan 2011, Chondrogenesis in perfusion bioreactors using porous silk scaffolds and hESC-derived MSCs, *Journal of Biomedical Materials Research Part A* **96A**(1): 21-28.

Truscello, S., G. Kerckhofs, S. Van Bael, G. Pyka, J. Schrooten and H. Van Oosterwyck 2012, Prediction of permeability of regular scaffolds for skeletal tissue engineering: A combined computational and experimental study, *Acta Biomaterialia* **8**(4): 1648-1658.

Van Bael, S., G. Kerckhofs, M. Moesen, G. Pyka, J. Schrooten and J. P. Kruth 2011, Micro-CT-based improvpeement of geometrical and mechanical controllability of selective laser melted Ti6Al4V porous structures, *Materials Science and Engineering a-Structural Materials Properties Microstructure and Processing* **528**(24): 7423-7431.

van Gastel, N., M. Depypere, I. Stockmans, J. Schrooten, F. Maes, F. P. Luyten and G. Carmeliet 2012a, Interactions between periosteal cells and blood vessels during bone autograft healing: implications for tissue engineering strategies, *Journal of Tissue Engineering and Regenerative Medicine* **6**: 310-310.

van Gastel, N., S. Torrekens, S. J. Roberts, K. Moermans, J. Schrooten, P. Carmeliet, A. Luttun, F. P. Luyten and G. Carmeliet 2012b, Engineering Vascularized Bone: Osteogenic and Proangiogenic Potential of Murine Periosteal Cells, *Stem Cells* **30**(11): 2460-2471.

Zhou, X., I. Holsbeeks, S. Impens, M. Sonnaert, V. Bloemen, F. P. Luyten and J. Schrooten 2013, Non-invasive real-time monitoring by alamarBlue(R) during in vitro culture of 3D tissue engineered bone constructs, *Tissue Eng Part C Methods* **19**(9): 720-729.

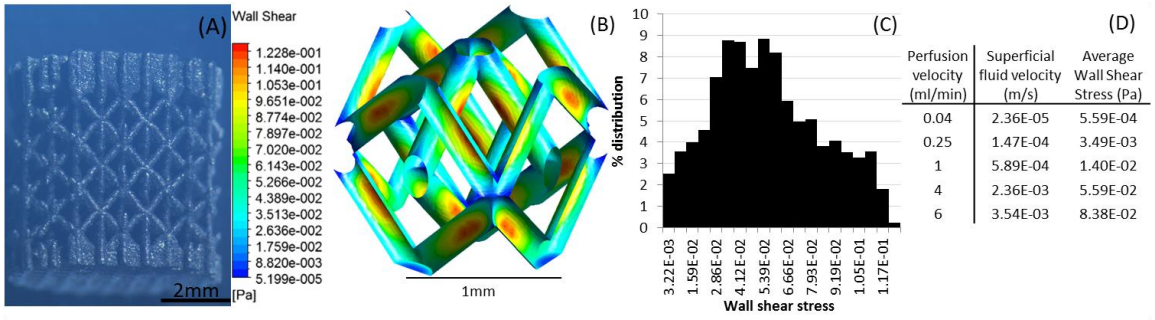

FIG. 1.: (A) Bright field image of a Ti6Al4V scaffold, (B) SS distribution on a scaffold unit cell for a perfusion velocity of 4 ml/min, (C) relative distribution of the SS on the scaffold unit cell for a perfusion velocity of 4 ml/min and (D) interstitial fluid velocity and average SS corresponding with the applied perfusion velocities. All calculations were performed on an empty scaffold, thus representing the initial SS present after cell attachment and prior to construct culturing.

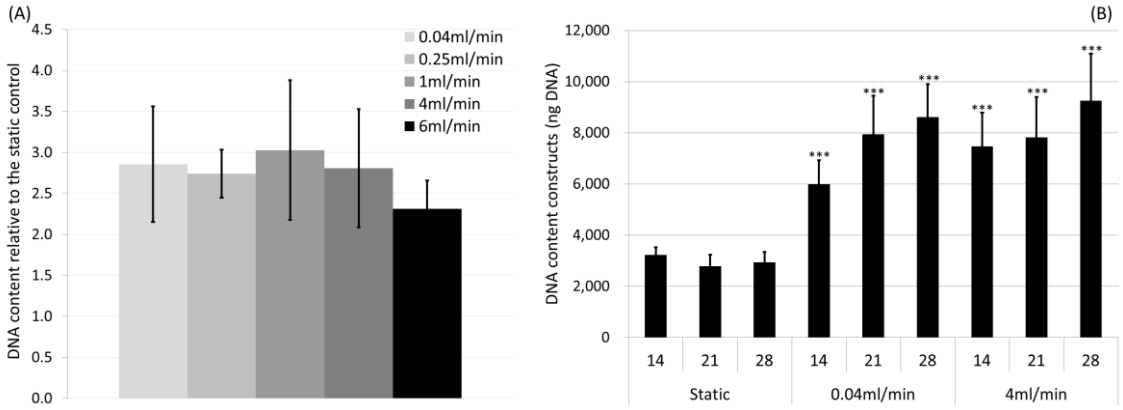

FIG. 2. (A) DNA content of the constructs relative to the static control after 3 weeks of dynamic culture (n=4 to 6), (B) DNA content of the constructs after 14, 21 or 28 days of culture in a static or perfused (0.04 ml/min and 4 ml/min) system (n=4, ***p<0.001, black bars show standard deviations of the mean).

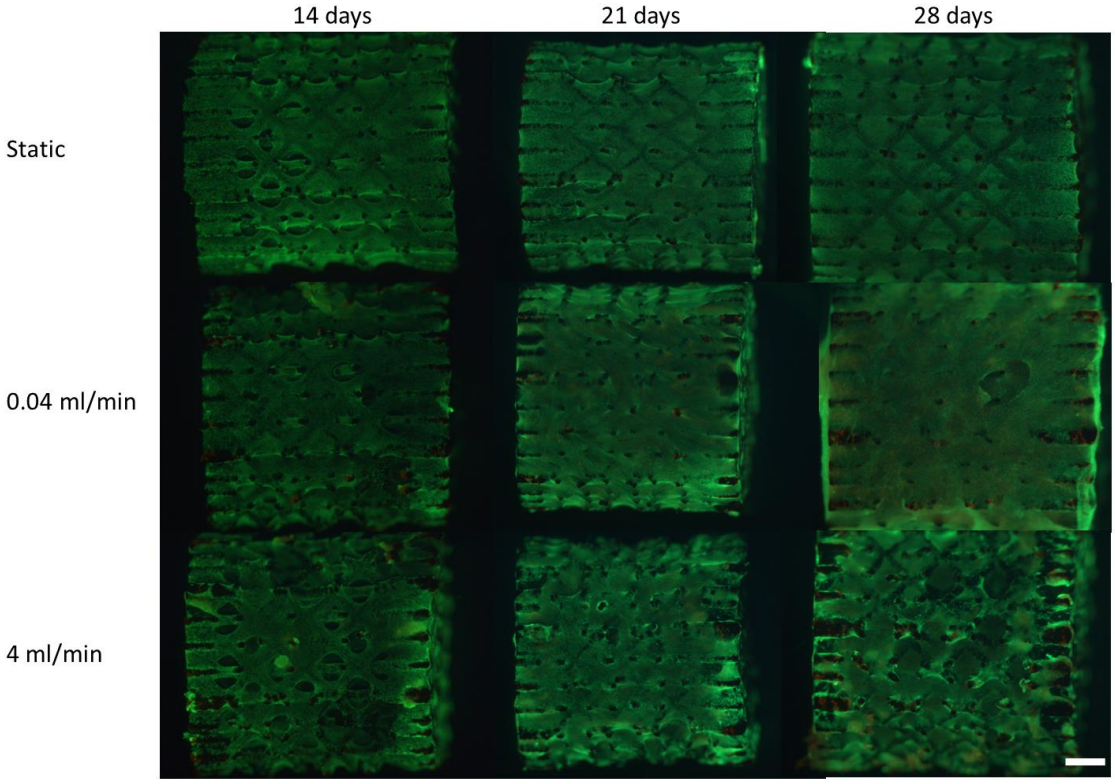

FIG.3. Live/Dead staining of constructs for different culture regimes and durations. The green fluorescent dye shows all the living cells while the red dye visualises the nuclei of the dead cells. Scale bar is 1mm

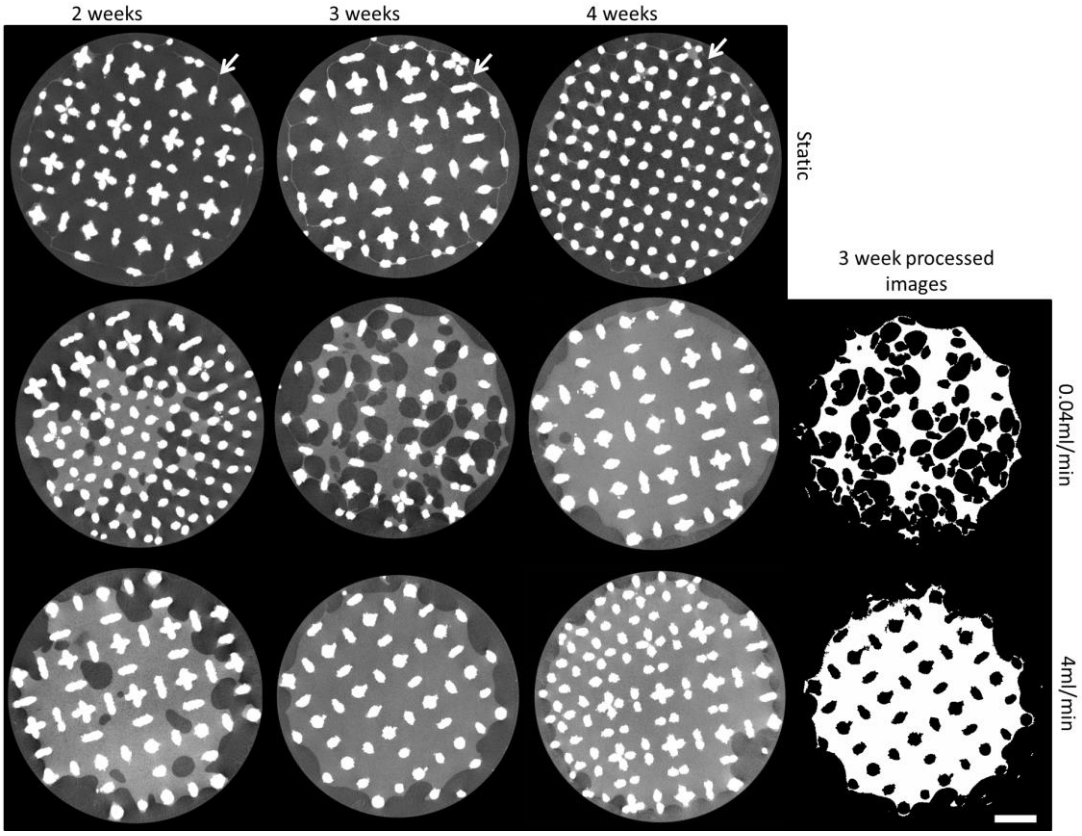

FIG.4. Representative 2D CE-nanoCT cross-sectional images stained with Hexabrix® of the constructs cultured at different conditions and their corresponding processed images for 3 weeks of perfusion culturing. White arrows indicate cell-matrix in the static conditions. Scale bar is 1mm.

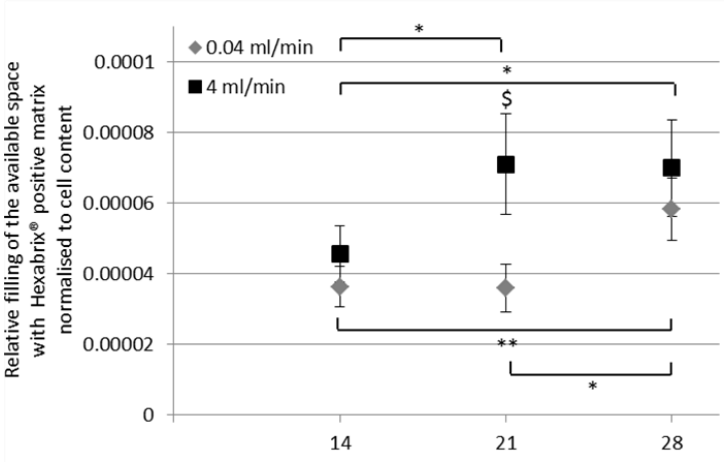

FIG.5. Relative filling of the scaffold determined with Hexabrix® normalised to cell content, $ indicates a significant difference between the two flow rates ($p<0.05$), *: $0.05>p>0.01$, **: $0.01>p>0.001$

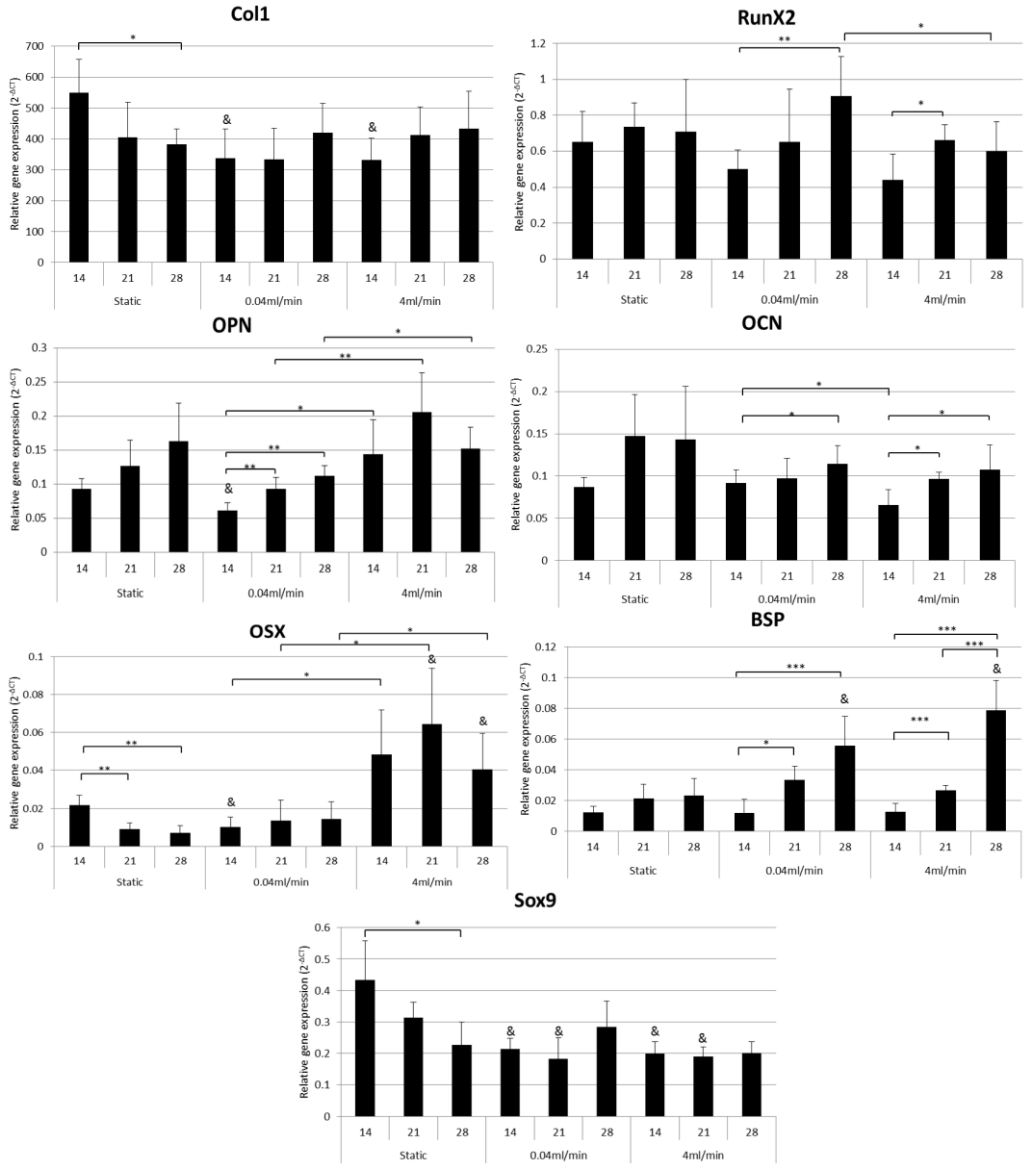

FIG.6. Gene expression of the cultured constructs by means of RT PCR for Col1, RunX2, OPN, OCN, BSP, Sox9 and OSX relative to HPRT. & indicates a significant difference with the corresponding time point of the static control ($p<0.05$), *: $0.05>p>0.01$, **: $0.01>p>0.001$. (n=4).

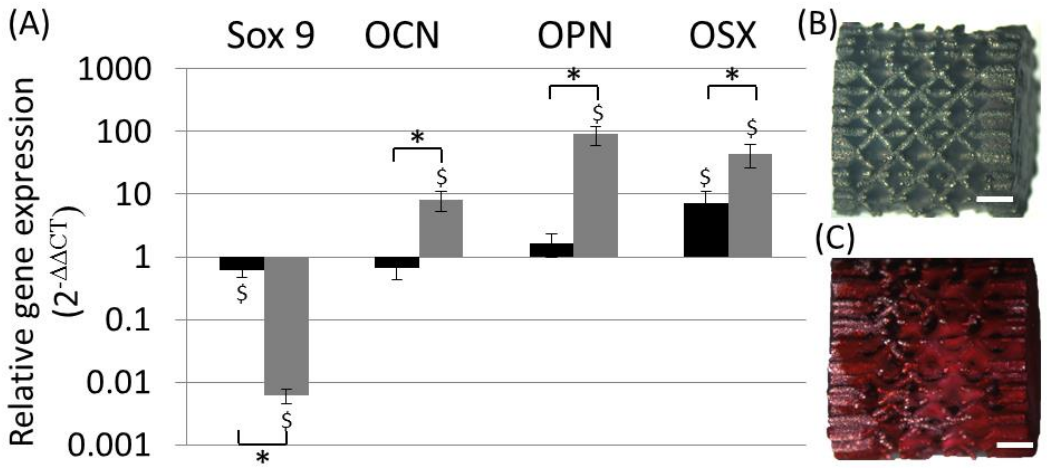

Fig.7. (A) Gene expression of perfusion bioreactor cultured constructs with normal growth medium (Black) and mineralisation medium (Grey) for 21 days relative to HPRT and to the static control (ΔΔCT) by means of RT PCR for Sox9, OCN, OPN and OSX. $ shows relative to the static control. $P<0.05$, n=3 (B and C) Alizarin red staining of respectively normal growth medium and mineralisation medium cultured constructs after 21 days of culture. Scale bars are 1 mm